Journal of Sustainable Development of Natural Resources Management

http://www.sdewes.org/jsdnarema

Year XXXX, Volume X, Issue Y, xxxxxx

Original Research Article

Impact of Fuel Cell Stack Configuration on the Energy Efficiency of Hybrid Electric Vehicles: A MATLAB/Simulink-Based Simulation

ABSTRACT

This study evaluates the system-level performance of a fuel cell hybrid electric vehicle (FCHEV) using a dynamic simulation framework. The powertrain integrates a proton-exchange membrane fuel cell, a battery pack, and an electric traction motor to enable efficient power sharing across varying driving demands. A supervisory energy-management strategy regulates power flow between the fuel cell and the battery based on load requirements, with the fuel cell supplying base power and the battery supporting transient acceleration events. Simulations were conducted for 300-, 500-, and 600-cell stack configurations. The results show that increasing the stack size from 300 to 500 cells improves fuel economy and reduces hydrogen consumption. In contrast, the additional gain from 500 to 600 cells is smaller, indicating diminishing returns beyond 500 cells. Hydrogen consumption is reported together with the battery state of charge (SOC) at the beginning and end of the driving cycle to confirm that the observed efficiency gains are not driven by net battery energy depletion. Overall, the proposed modeling approach provides a reproducible basis for evaluating design trade-offs in fuel cell hybrid powertrains and supports future clean-mobility applications.

KEYWORDS

cell-count sensitivity; supervisory energy management; power-split control; hydrogen consumption; state-of-charge tracking; balance-of-plant losses; standardized driving cycles; semi-empirical fuel-cell modeling

1. INTRODUCTION

The transportation sector is a leading contributor to global greenhouse gas emissions due to its reliance on fossil fuels [1]. In recent years, FCEVs have emerged as a sustainable alternative to internal combustion engine (ICE) vehicles, using hydrogen to generate electricity via electrochemical reactions in a fuel cell stack [2]. Compared to battery-electric vehicles (BEVs), FCEVs offer several potential advantages, including shorter refueling times and longer driving ranges, making them suitable for broader transportation needs [3].

However, several barriers continue to slow their adoption, such as the high cost of fuel cell components, limited hydrogen infrastructure, and challenges in hydrogen production and storage [4]. These limitations highlight the need for efficient system modeling to optimize vehicle performance and inform infrastructure development strategies [5,6].

In recent decades, the transportation sector's adverse environmental effects and the US's dependency on petroleum have been top concerns. Because non-renewable fossil fuels are running out, the existing energy landscape is unsustainable and leads to environmental problems, including the greenhouse effect [7, 8].In order to improve system performance and

overall efficiency, recent research has investigated the integration and optimization of hydrogen-based hybrid energy systems [9].

Battery-electric vehicles (BEVs) offer superior energy efficiency; however, they are hindered by long charging times and limited driving range due to battery size limitations. Conversely, FCEVs offer extended range, rendering them more appropriate for applications that require uninterrupted operation [10].

However, despite their potential, several technological, economic, and infrastructural challenges limit the widespread adoption of FCEVs. The high cost of fuel cell components, limited hydrogen production and storage capabilities, and the lack of refueling infrastructure are significant barriers that must be addressed through continued innovation and coordinated policy efforts.

The vehicle can be propelled directly by the fuel cell's rotational energy or transformed into electrical energy using a generator. A fuel cell uses an ecologically acceptable mechanism to directly convert chemical energy into electrical energy, just like an internal combustion engine (ICE) does [11–16]. Unlike batteries, which gradually deplete during use, internal combustion engines and fuel cells run continuously as long as fuel is available [17]. Consequently, hydrogen fuel cells are projected to overcome the limitations of battery-electric vehicles, positioning hydrogen as a leading contender for the future of transportation fuels.

.

The current research builds upon existing literature but seeks to provide a more integrated perspective by combining theoretical foundations, technological developments, and simulation-based performance evaluation. Specifically, the study investigates the principles of fuel cell operation, hybrid powertrain configurations, and various hydrogen storage methods. Furthermore, a detailed simulation model in MATLAB/Simscape is developed to analyze the dynamic behavior of fuel-cell hybrid electric vehicles under real-world driving conditions.

The goal of this study is to fill this gap by developing a detailed simulation model of a fuel-cell hybrid electric vehicle (FCHEV) in MATLAB/Simulink. This study differs from previous ones that only examined subsystems. It shows a fully integrated vehicle simulation that tests how design choices, including the number of fuel cells and motor control algorithms, affect the system's overall efficiency in real-world driving. The results help us understand how FCHEVs work and offer ideas for improving future clean transportation systems.

Innovations and contributions. This study does not assert originality in hybridization, despite the commercial maturity of hybrid electric powertrains. It offers a system-level, reproducible modeling and sensitivity framework for fuel-cell hybrid electric vehicles (FCHEVs) that measures the influence of fuel-cell stack scaling on overall vehicle performance. The suggested MATLAB/Simulink–Simscape model incorporates the fuel cell stack, battery pack, power electronic converters, traction motor, drivetrain/road-load dynamics, and a supervisory energy management technique. We assess the impact of varying stack size on power distribution, hydrogen consumption, state-of-charge progression, and peak component loading using standardized driving cycles. This facilitates uniform comparison among stack configurations and underpins evidence-based decisions about stack sizing.

It should be mentioned that hybrid electric vehicle technologies are already commercially developed in a variety of configurations in order to better place this work in relation to the present state of the art. However, internal combustion engines are the main source of power in the majority of commercially available mild-hybrid systems, with batteries merely acting as a supplementary component. The current study, on the other hand, looks at a hydrogen fuel-cell-dominant hybrid architecture where the battery handles transient power demands and regenerative energy recovery while the PEM fuel cell supplies the main propulsion power. The

system-level assessment of fuel-cell stack scaling (300, 500, and 600 cells) and its impact on vehicle-level performance metrics including MPGe, hydrogen consumption, and battery state-of-charge stability under standardized driving cycles is what makes this study novel. This approach provides a replicable framework for examining FCHEV design trade-offs at the vehicle level.

2. Literature Review

2.1 Hydrogen as a Fuel for Vehicles

The production cost of hydrogen, being a synthetic fuel, is approximately three times that of oil refining [18]. Substantial initiatives are underway to develop an efficient, sustainable method for hydrogen production for vehicle engines. Automakers, including Hyundai, Toyota, and Honda, are now producing hydrogen-powered fuel cell vehicles (FCVs). Presently available in North America, Asia, and Europe, these fuel cell vehicles have predominantly been acquired by early adopters.

The majority of contemporary consumers are educated, live in larger residences, earn higher incomes, are open to life changes, and share common traits [19]. Battery Electric Vehicles (BEVs) and Fuel Cell Vehicles (FCVs) use electric motors, rely on sustainable, renewable energy sources, and produce no exhaust pollutants. The two principal distinctions between BEVs and FCVs are operational range and refueling method—fuel cell vehicles (FCVs) with a range exceeding approximately 480 km. The driving range is comparable to that of a conventional fossil-fuel vehicle, as it can be replenished at a hydrogen filling station in less than 10 minutes. Battery Electric Vehicles (BEVs) and Fuel Cell Vehicles (FCVs) share commonalities in their electric propulsion systems, the absence of tailpipe emissions, and their dependence on renewable and sustainable energy sources. The primary differences between BEVs and FCVs are driving range and refueling technique. The range of fuel cell vehicles exceeds approximately 480 km.

The prospects for hydrogen as a fuel are more favorable. Fuel cell prices are anticipated to match those of internal combustion engines by 2030, contingent upon availability and future technology improvements [19]. A primary obstacle to the extensive adoption of hydrogen is the necessity for improved storage solutions. Due to its low density, hydrogen poses greater storage challenges than other fossil fuels.

A further potential drawback is the public's apprehension regarding the utilization of high-pressure (70 MPa) storage tanks in automobiles. [20] Research is currently underway on a tank with an internal skeleton—an elaborate arrangement of struts designed to withstand the pressures of compressed gas—as a potential alternative to conventional CH2 tanks.

Liquid hydrogen storage (LH2) has advanced significantly and currently offers the highest specific mass (15%) among all hydrogen storage techniques for automobiles; however, using liquid hydrogen results in lower energy efficiency [21]. The boil-off problem must be addressed before the extensive implementation of LH2 systems. An alternative concept is a cryo-compressed tank that uses cryogenic temperatures to achieve enhanced hydrogen compression. Hydrogen may be extracted from several sources, including water, hydrogen sulfide, and hydrocarbon fuels [23].

Hydrogen cannot be synthesized from its components without external energy sources, such as thermal, electrical, photonic, and biological energy. Ammonia decomposes into hydrogen and nitrogen aboard; hence, it has been proposed as a fuel for internal combustion engines [24, 25]. Ammonia is a chemical substance distinguished by a high concentration of hydrogen. Hydrogen can be produced using both non-renewable and renewable energy sources. Greenhouse gases (GHG) are released during hydrogen synthesis from non-renewable sources.

Nevertheless, hydrogen produced from renewable sources is constantly environmentally neutral [26, 27].

The electrochemical generation of hydrogen from waste biomass is a method that produces no greenhouse gas emissions, requires minimal energy, and incurs low manufacturing costs. Potential biomass feedstocks include cypress sawdust, rice chaff, and bread crumbs [28, 29]. Likewise, newspapers can be electrolyzed to produce hydrogen directly. In the solvent H3PO4, newsprint, comprising 69.2% cellulose and 11.8% lignin, undergoes degradation similar to electrolysis, producing monosaccharides, disaccharides, and aliphatic keto acids [30, 31]. Hydrogen can also be produced by electrolyzing humidified methane [32].

2.2 FCVs' Storage of Hydrogen

Storing sufficient hydrogen is a critical area of research for the development of fuel cell vehicles (FCVs). Because hydrogen has a low energy density, fitting enough fuel for a practical driving range into a car without making the storage system excessively large or heavy is a significant challenge. Therefore, innovative hydrogen storage technologies are being developed to meet consumer expectations. Figure 1 shows an example of an FCV using compressed gas storage and provides a general survey of different hydrogen storage approaches [33].

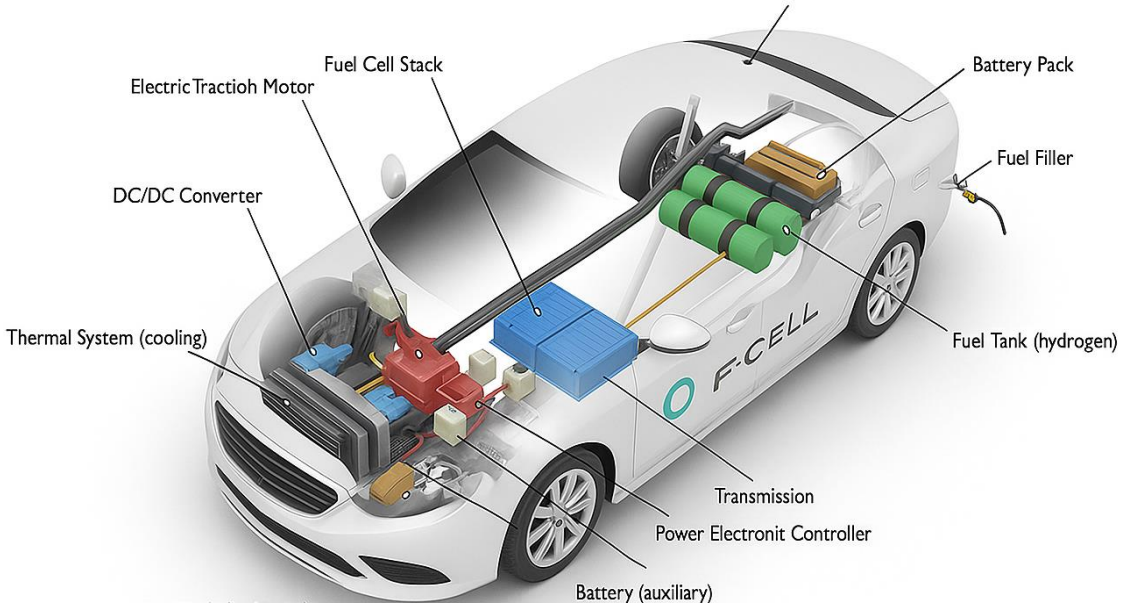

Figure 1. On-board storage in a fuel cell car [33]

2.3 Fuel Cell Technologies for Transportation

Fuel cells convert hydrogen and oxygen into energy via electrochemical reactions and are highly efficient, with low emissions. Although there are several fuel cell technologies, such as Alkaline Fuel Cells, Phosphoric Acid Fuel Cells, and Solid Oxide Fuel Cells, they typically share the same drawbacks: CO_2 sensitivity, slow thermal response, and high operating temperatures, limiting their use in automotive applications [34]. Meanwhile, Proton Exchange Membrane Fuel Cells (PEMFCs) have become the leading technology for transportation because they operate at low temperatures (60–80 °C), can be quickly started, and offer high power density and good transient response to changing vehicle loads [35]. Performance is managed through the limitations of activation losses, ohmic resistance, membrane hydration, catalyst degradation, and reactant mass-transport limitations, all of which should be appropriately managed to enable stable, long-term operations [36], [37]. The following project will focus solely on PEMFC systems as the primary energy source for propulsion in FCHEV topologies under real-world driving conditions.

2.4 Principles of Fuel Cell

Fuel cell (FC) systems, despite their diversity as shown in Table 1, all adhere to a common operating principle. Each fuel cell has three fundamental components: an anode, a cathode, and an electrolyte that separates them. Fuel cells are categorized by the type of electrolyte used. Each cell encompasses these three essential components, regardless of whether it includes hundreds of separate cells. Figure 2 illustrates a standard operating flowchart for a polymer electrolyte membrane fuel cell (PEMFC), also known as a PEMFCs . PEMFCs are familiar power sources for portable devices, particularly in cars[38]. In a PEMFC, hydrogen fuel is delivered to the anode, and air or pure oxygen is provided to the cathode.

The specific electrolyte used depends on the type of fuel cell. At the anode, hydrogen gas is dissociated into electrons and hydrogen ions. The membrane is a barrier that allows only hydrogen ions to traverse to the cathode. Hydrogen ions react with oxygen atoms to generate water (H_2O) while generating heat [39]. A fundamental distinction between fuel cells (FCs) and internal combustion engines is their operational processes: FCs amalgamate fuel and oxidants without combustion, while engines combust them simultaneously. This difference elucidates why fuel cells generate no harmful pollutants compared to internal combustion engines.

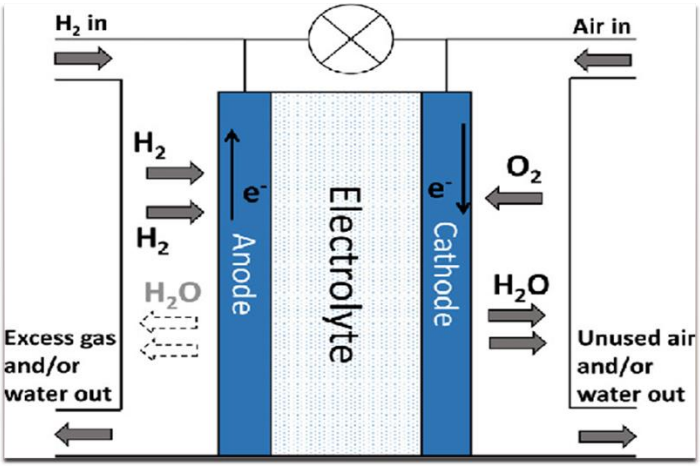

Figure 2. The principle of fuel cell operation

Table 1 Comparison of the operating temperatures and stack voltage efficiency of several Fuel Cell types [44]

Type	*Temperature of operation*	*Efficiency of stack voltage*	*advantages*	*disadvantages*
Solid oxide Fuel Cell (SOFC)	*> 700◦C*	*60%-80%*	*high operational pressure, reused heat, and efficiency*	*Limited commercialization and poor maturity.*
Phosphoric acid fuel cell (PAFC)	*Around 180◦C*	*Over 80%*	*high cogeneration efficiency for heat.*	*High catalyst costs and poor current density are issues.*
Alkaline Fuel Cell (AEFC)	*< 80◦C*	*62% - 82%*	*excellent durability and maturity*	*limited range of partial loads and low current density*

2.5 FCEVs Opportunities & Challenges

Fuel Cell Electric Vehicles (FCEVs) are a perfect solution for eco-friendly and efficient transportation. They come with long-range drives, quick charging times, and steady power even during heavy or high-temperature driving. FCEVs produce only water vapor during operation. Fuel cell electric vehicles (FCEVs) offer extended range and rapid refueling, advantages over battery electric vehicles (BEVs) for long-distance travel. However, many problems still block the broader use of such vehicles. The high cost of fuel-cell stacks, durability issues under dynamic loading, and the lack of hydrogen refueling infrastructure are the main bottlenecks.

Besides, hydrogen production, storage, and transportation are still a long way from meeting the economic and technological requirements for large-scale deployment. These are the very problems that need a solution for the extensive use of FCEVs within the future mobility environment that would be viable for sustainable development.

2.6 Hybridization of Fuel Cell Powertrains

Modern fuel cell vehicles include a number of safety features, such as shut-off valves, pressure relief systems, reinforced high-pressure storage tanks, and hydrogen leak detection sensors, despite the fact that hydrogen is combustible. In addition, hydrogen is substantially lighter than air and disperses swiftly in open spaces, which decreases the possibility of harmful accumulation. Therefore, appropriate tank design, ventilation, and established vehicle safety requirements reduce the risks associated with hydrogen.

2.7 Hybridization of Fuel Cell Powertrains

The combination of fuel-cell powertrains and energy storage brings significant improvements to the vehicle's overall efficiency, response time, and even the lifetimes of its components. In regular (FCHEV) technologies, the fuel cell supplies steady-state power for cruising, while the battery or supercapacitor handles rapid power changes for acceleration and regenerative braking. This power-sharing technique diminishes rapid load changes on the fuel-cell stack, alleviating degradation mechanisms and enhancing durability [1]. Moreover, hybridization allows the fuel cell to operate close to its peak efficiency. At the same time, the battery recovers braking energy and meets high-power requirements, thereby enhancing total energy efficiency and reducing hydrogen consumption [2]. Advanced energy management techniques (EMS), encompassing rule-based and optimization-based methodologies, enhance system performance by regulating power flow among subsystems under diverse operational conditions [3]. Consequently, hybrid fuel-cell architectures have emerged as the optimal choice for contemporary FCHEVs, offering enhanced performance, improved load management, reduced fuel consumption, and greater long-term reliability [4].

Furthermore, the SOC profiles remained same across the evaluated stack configurations, indicating that the trends in hydrogen consumption were not due to net battery depletion. Overall, the simulation results demonstrate that increasing the stack size from 300 to 500 cells increases fuel economy and reduces hydrogen consumption; however, the further benefit at 600 cells is negligible, indicating diminishing returns beyond the 500-cell configuration.

2.7 Research Gap

Furthermore, the SOC profiles remained same across the evaluated stack configurations, indicating that the trends in hydrogen consumption were not due to net battery depletion. Overall, the simulation results demonstrate that increasing the stack size from 300 to 500 cells increases fuel economy and reduces hydrogen consumption; however, the further benefit at 600 cells is negligible, indicating diminishing returns beyond the 500-cell configuration.

The majority of early studies focused on the separate analysis of components of FCHEV powertrains rather than on evaluating a fully integrated system under realistic driving conditions. Besides that, only a few studies have examined the effects of fuel-cell stack scaling—the 300-cell vs. 500-cell configuration—on energy efficiency, MPGe performance, and power distribution. This research addresses this shortcoming by conducting a thorough MATLAB/Simulink simulation of an FCHEV architecture.

3 Methodology

The research focuses on a simulation-based approach to determine how well-performing PEMFCs perform under different driving conditions. The method employs a combination of fuel-cell electrochemical modeling, vehicle powertrain modeling, and energy management strategies within a single MATLAB/Simulink framework. The simulation starts with the development of a semi-empirical PEMFC model that faithfully captures generator voltage, hydrogen production, and temperature effects. The entire FCHEV powertrain, including the

battery pack, DC/DC converter, traction inverter, and motor, is built using a modular block-based architecture. Power-sharing features, stack loading, and dynamic hydrogen consumption are assessed using standardized driving cycles (NEDC, WLTC, and UDDS). Eventually, a two-stack configuration (300 vs. 500 cells) is compared to determine the impact of stack size on efficiency, transient performance, and fuel economy. This approach provides a consistent, reproducible platform for assessing FCHEV performance in real-world traffic conditions.

4 System Architecture of the FCHEV

A FCHEV comprises multiple subsystems that collaboratively ensure effective power generation, energy storage, and propulsion. The PEMFC constitutes the system's most critical component. It converts hydrogen and oxygen into electricity via an electrochemical reaction, producing only water and heat as byproducts. The fuel cell stack generates direct current (DC) electricity, which is either used immediately to power the electric motor or stored in a lithium-ion battery for later use. During braking, regenerative energy is recovered and stored in the battery.

A control system continuously monitors parameters such as power demand, SOC, and fuel cell performance to regulate energy flows effectively. It dynamically adjusts power allocation between the fuel cell and the battery to achieve optimal, efficient vehicle operation. The electric motor driving the wheels receives power from an inverter that converts the DC output from the fuel cell and batteries into AC.

The architecture includes supporting subsystems, such as thermal management units that maintain optimal temperatures for the fuel cell and batteries, and hydrogen storage tanks capable of withstanding high pressure. These tanks deliver a continuous flow of hydrogen to the fuel cell, ensuring its optimal operation.

Figure 3 shows the FCHEV system architecture, which has multiple energy sources and power-conditioning devices incorporated to provide efficient and reliable propulsion. The fuel-cell stack is the primary source of continuous power; its energy is passed through a DC/DC converter to smooth the voltage, then to the DC bus. A high-voltage battery is placed in the circuit to provide extra power for very short-term events, such as going fast, and to recover energy during regenerative braking. The inverter converts the DC bus voltage to AC power that the traction motor needs to produce torque to move the vehicle. Auxiliary devices are used for balance-of-plant operations such as supplying air, cooling, and regulating power electronics. This architecture enables synchronized power distribution, which, on the one hand, allows the fuel cell to operate at its maximum efficiency near its capacity. On the other hand, the battery handles load variations and energy recovery, resulting in better overall performance and lower hydrogen consumption.

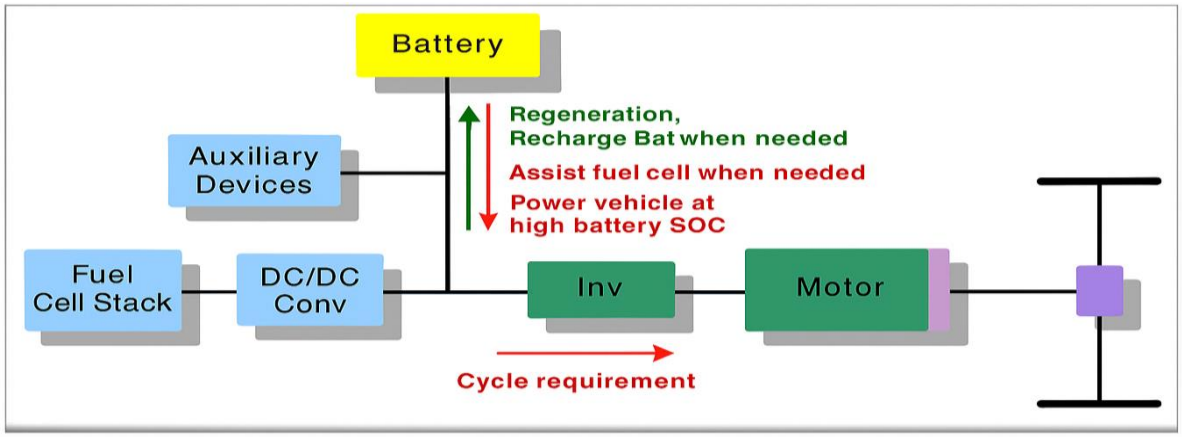

Figure 3. System architecture of FCHEV, showing the interaction between the fuel-cell stack, battery, DC/DC converter, inverter, and traction motor.

5 Fuel Cell Modelling

5.1 PEMFC Voltage Model

The PEMFC converts the chemical energy of hydrogen and oxygen to electrical energy via electrochemical reaction - as depicted in Fig. 1 2. The fundamental component of the PEMFC is a proton-conducting polymer electrolyte membrane that prevents electron movement. The anode is supplied with hydrogen, which is then split into protons and electrons [44,45]. The electrons then must travel through an external circuit to generate electric power, and the protons pass through the membrane to the cathode, where they react with oxygen to form water (and heat). A single PEMFC cell typically generates 0.9–1.23 V; therefore, multiple cells ($(N_{\text{cells}}$) They are connected in series to form a stack, and the total voltage is calculated as:

$$V_{\text{stack}} = N_{\text{cells}} \times V_{\text{cell}} \quad (1)$$

The actual cell voltage deviates from the ideal value due to several loss mechanisms, and is expressed as:

$$V_{\text{cell}} = E_{\text{Nerנst}} - (v_{\text{act}} + v_{\Omega} + v_{\text{con}}) \quad (2)$$

The reversible open-circuit voltage $\boldsymbol{E}_{\text{Nernest}}$ Is derived from the Nernst equation:

$$\boldsymbol{E_{Nernest} = 1.229 - 85 \times 10^{-5}(T - 298.15) + 4.3085 \times 10^{-5} \times T\left(ln\left(P_{H2}\sqrt{P_{O2}}\right)\right)} \quad (\mathbf{3})$$

The activation overpotential is modeled as:

$$V_{act} = -[\xi_1 + \xi_2 T + \xi_3 T \times \ln(C_{o2}) + \xi_4 T \times \ln(I)] \quad (4)$$

The ohmic voltage loss is expressed as:

$$\boldsymbol{V_{\Omega} = I(R_m \times R_c), R_m = \frac{\rho_m \times l}{A}} \quad (\mathbf{5})$$

Finally, concentration losses are computed as:

$$\boldsymbol{V_{\text{con}} = -\beta ln\left(1 - \frac{J}{J_{max}}\right) == -\beta\, ln\left(1 - \frac{\frac{I}{A}}{J_{max}}\right)} \quad (6)$$

Consequently, the resulting model delivers a numerically reliable and physically coherent depiction of PEMFC performance across diverse operating situations.

Where:

- T = Cell operating temperature (K)
- I = Cell current (A)
- A = Active membrane area (cm²)
- PH_2, PO_2 = Partial pressures of hydrogen and oxygen (atm)
- λ = Membrane water content

- β = Concentration loss coefficient
- $\xi_1 - \xi_4$ = Activation-loss empirical constants

5.2 Hydrogen Consumption Model

Hydrogen consumption in the PEMFC rises in direct correlation with the stack current. According to Faraday's law, the molar hydrogen flow rate is directly proportional to the electrochemical reaction rate, indicating that an increased current demand necessitates a correspondingly elevated hydrogen supply. In realistic FCHEV simulations, the unrefined hydrogen flow is adjusted using efficiency and purge-loss ratios to accurately reflect actual operating conditions.

5.3 Stack Thermal Model

The stack temperature is determined by the balance between the heat produced by the exothermic electrochemical reaction and the heat removed by the stack cooling system. The temperature increases as the activation and ohmic losses dissipate, the two main components of the heat released during the power generation phase. A coolant loop is used to maintain a constant temperature, keep the membranes moist, and prevent deterioration. The temperature of the stack has to be kept in (60-80 °C) for optimum output, efficiency, cycle-to-cycle stability, and longevity under all operating conditions.

5.4 Operating Constraints

However, certain physical and operational constraints may be introduced into the PEMFC model to ensure it operates safely, stably, and effectively within the FCHEV framework, avoiding membrane degradation, overheating, reagent depletion, and excessive hydrogen losses during transient driving conditions.

1. Voltage Limitations

Cell voltage must be controlled to prevent membrane dehydration at high voltage or catalyst damage at very low voltage.

2. Current Limitations

The current density is limited by the membrane surface area, diffusion, and cooling to prevent reactant depletion and thermal degradation.

3. Temperature Limits

The stack must operate within a specific temperature range (typically 60-80 °C) to maintain membrane hydration and ensure acceptable proton conductivity.

4. Pressure and Humidity Conditions

Maintaining proper partial pressures of hydrogen and oxygen, and a controlled relative humidity, is also essential to ensure reaction stability while avoiding problems such as flooding or membrane drying.

5. Hydrogen Utilization Limit

Hydrogen is typically used only partially (e.g., 80–95%) to provide an excess of hydrogen at the anode, thereby improving stability and preventing nitrogen formation.

Together, these limitations ensure the real-world functionality of PEMFCs and maintain long-term durability when integrated into an FCHEV powertrain.

6. Simulation Setup and Driving Conditions

The FCHEV model was developed in MATLAB/Simulink with a modular architecture that incorporates the PEMFC stack model, lithium-ion battery, DC/DC converter, traction inverter, and motor drive. All subsystems were set to function under realistic vehicle load fluctuations to assess system performance, hydrogen consumption, and power-sharing dynamics.

6.1 Model Development

Further details of the Simulink/Simscape implementation are provided in Appendix A.

6.2 Simulation Architecture

The simulation framework has the following components:

- The PEMFC stack model employs the semi-empirical voltage and hydrogen consumption equations outlined in Section 4.
- Battery Pack: provides temporary power during acceleration and captures energy from regenerative braking.
- DC/DC Converter: regulates power transfer among the fuel cell, battery, and DC bus.
- Traction Inverter and Motor: transform electrical energy into mechanical torque for propulsion.
- The Supervisory Energy Management System (EMS) regulates the real-time power distribution between the PEMFC and battery to optimize hydrogen usage and maintain fuel cell longevity.

All component data and rated parameters (voltage, capacities, efficiency, etc.) were derived from values documented in commercial FCHEV platforms and scholarly literature.

6.3 DrivprimaryCycles

Real-world conditions were the primary criterion for assessing the FCHEV system's performance; thus, various standardized driving cycles were used. These cycles were:

- NEDC (New European Driving Cycle): characterized by soft accelerations and low-speed urban driving conditions.
- WLTC - Worldwide Harmonized Light Vehicles Test Cycle: This cycle has fast acceleration, different speed stages, and varying load as prominent features.
- UDDS (Urban Dynamometer Driving Schedule): simulated urban driving with stop-and-go conditions, creating high transient power requirements.

The cycles allow the determination of hydrogen consumption, fuel-cell efficiency, power distribution, and thermal dynamics under different loading conditions.

6.4 Simulation Model Description

A simulation model was constructed in MATLAB/Simulink and Simscape to assess the dynamic behavior and energy efficiency of the proposed FCHEV. The model encompasses all critical elements of an FCHEV, including a PEMFC, a lithium-ion battery, an electric traction motor, and a supervisory control unit that regulates power distribution and ensures system safety.

The PEMFC subsystem models the electrochemical transformation of hydrogen into electricity. It is configured according to standard commercial stack characteristics, encompassing cell area, cell quantity, membrane thickness, and temperature range. The fuel cell model computes output voltage and current based on load demand, reactant availability, and operating circumstances. The battery unit enhances the fuel cell by supplying more power during acceleration and storing surplus energy during regenerative braking. A lithium-ion battery model was employed, characterized by its nominal voltage, capacity, and state-of-charge dynamics. The inverter converts DC power from the battery and fuel cell into AC power to operate the motor. The electric motor module replicates vehicle propulsion. It encompasses torque-speed characteristics and efficiency maps, and facilitates bidirectional operation—propulsion during acceleration and energy recuperation during braking. The motor is linked to a streamlined powertrain and vehicle body model that considers vehicle mass, drag force, rolling resistance, and road gradient.

A centralized control unit regulates the interaction among subsystems. It guarantees optimal power distribution between the fuel cell and the battery, maintains safe operating conditions, and regulates transitions between various driving modes. The control method uses real-time feedback on vehicle speed, battery SOC, and fuel cell status to inform power-flow decisions. Simulation inputs include a predetermined driving cycle, such as a conventional urban or highway speed profile, which facilitates the assessment of the vehicle's performance in realistic settings. Principal outputs encompass fuel cell power, battery current, motor torque, vehicle velocity, and total energy consumption. This integrated modeling approach provides a robust foundation for assessing performance, efficiency, and energy flow in FCHEVs, enabling evaluation of system-level enhancements through parameter variation and control strategy optimization.

Table 2: Fuel Cell Vehicle Model Parameters.

Fuel cell		
Electrolyte	***Area***	***280 cm²***
	Membrane Thickness	***0.01275 cm***
	Max current	***1.4 A/ cm²***
	Membrane Weight	***1.1 kg/mol***
	Number of cells	***400***
Anode	***Chamber Pressure***	***0.10132 MPa***
	Temperature	***80 °C***
	Cross-Sectional at Port A	***3.1416 cm²***
	Cross-Sectional at Port B	***3.1416 cm²***
	Cross-Sectional at Port C	***3.1416 cm²***
Battery		
	Part number	***AIM 12V7***
	Manufacturer	***A123***
	Battery type	***Lithium-ion***
	Capacity	***4600 (mAh)***
	V nominal	***13.2 (v)***

	Weight	***840 (g)***
	Height	***93.5 (mm)***
	Length	***151 (mm)***
	Width	***64.5 (mm)***
Vehicle Body		
	Chassis body	***1500 (kg)***
	Length	***1.624 (m)***
	Width	***1.2 (m)***
	Height	***0.4225 (m)***

The parameters in Table 2 are derived from standard values used in the design of fuel-cell hybrid electric vehicles (FCHEVs), with explicit sources and rationales provided for each. The parameters for electrolyte area, membrane thickness, and maximum current are obtained from conventional fuel cell design protocols and publications from reputable manufacturers. The cell count is tuned to vehicular power demands, as established through system-level simulations.Since PEM fuel cells normally function best in the 60–80 °C temperature range, the anode operating temperature was fixed at 80 °C. By operating close to the upper bound, the membrane's proton conductivity is enhanced and activation losses are decreased, increasing stack efficiency overall. Automotive PEM fuel cell systems frequently use this operating state, which is in line with values documented in the literature.

The selected chamber pressure and temperature for the anode are standard for high-efficiency fuel cells, guaranteeing optimal performance. The cross-sectional areas at ports A, B, and C conform to industry-standard fuel cell stack arrangements. The selected values were based on conventional stack designs, guaranteeing precise simulation of the electrochemical reactions in the fuel cell.

The battery characteristics are derived from the A123 lithium-ion battery, which is frequently used in electric automobiles due to its high energy density and reliability. The battery's capacity and nominal voltage were determined based on the vehicle's power requirements, while its weight, height, length, and width comply with the manufacturer's specifications for this model.

The vehicle body parameters, including chassis weight and dimensions, align with standard sizes for this class, as utilized in prior fuel cell vehicle simulations.

Fuel cell vehicles (FCVs), which emit zero tailpipe emissions and can potentially refuel more quickly than battery electric vehicles, offer a viable alternative to traditional gasoline-powered cars. The FCVs operate on pure hydrogen gas stored in an onboard tank, as seen in Figure 4, similar to the proposed concept. Refueling an automobile with hydrogen requires around three to five minutes, akin to refueling a vehicle with petrol. The fuel cell stack, which is the core component, is essential to a fuel cell vehicle (FCV). Figure 5 depicts the transfer of hydrogen from the tank to the fuel cell's anode (negative electrode). Figure 8 illustrates that oxygen from the ambient air is delivered to the fuel cell's cathode, or positive electrode. A catalyst, usually platinum, facilitates the chemical interaction between hydrogen and oxygen in the fuel cell. Water and energy are the products of this process. The electrochemical mechanism of the fuel cell generates electricity.

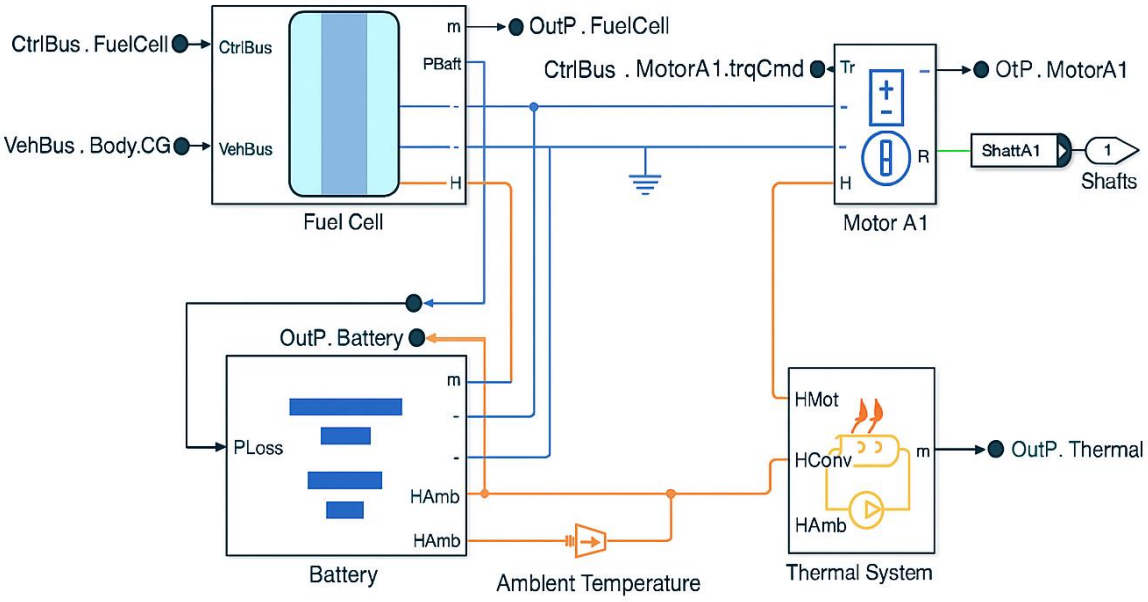

Figure 4. Structure Of Fuel Cell Vehicle.

This electricity powers the car's electric motor. The FCV is propelled by an electric motor similar to those used in battery-electric vehicles. A drivetrain and gearbox transmit the motor's power to the wheels. Water vapor is the only FCV emission released through the exhaust. A DC electrical network connects the battery and fuel cell to the motor. The control system determines the amount of electricity generated by the fuel cell and battery. The battery is recharged by feeding power back into it during braking actions. The battery, DC-DC converters, and motor temperature are all regulated by a thermal system represented by a fluid network. The weather outside is 27 degrees Celsius. A battery's SOC is a measurement and percentage that represents the energy available at any given time. As seen in Fig. 6, SoC shows how Much power is still in the cell.

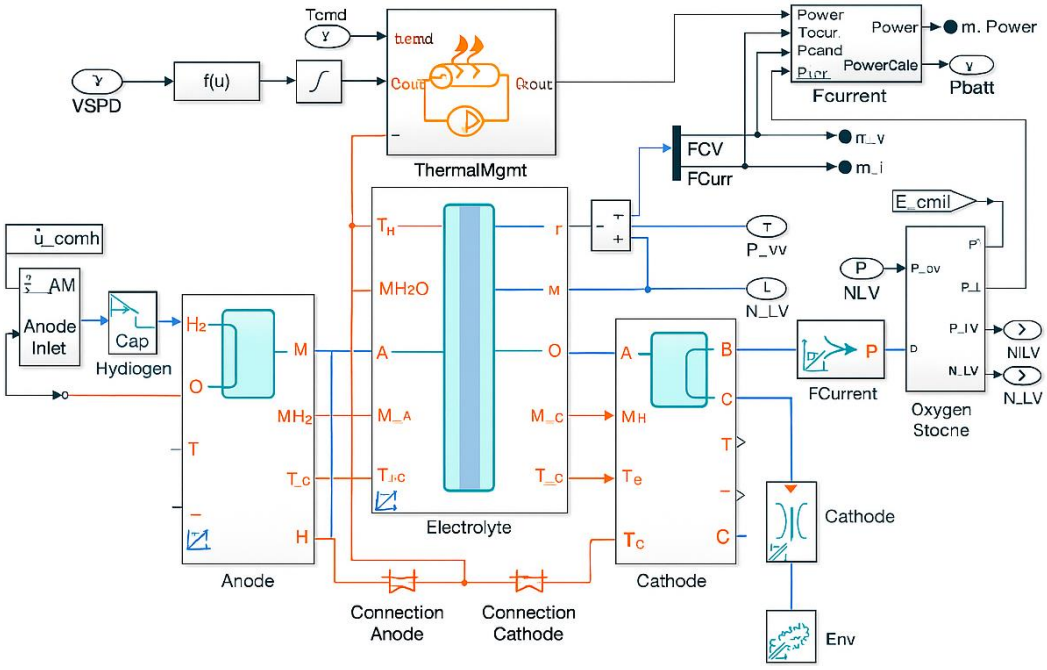

Figure 5. Electrochemical operating principle of the fuel cell.

Fig 5 is not meant to depict the entire FCHEV powertrain architecture, but simply the electrochemical working principle of the fuel cell. Fig 3 shows the entire vehicle-level system, including the fuel cell stack, battery, DC/DC converter, inverter, traction motor, and power flow interactions. The mechanical transmission line between the traction motor and the wheels in the drivetrain and vehicle dynamics subsystem of the simulation model represents the gearbox effect. The manuscript content has been updated to make the distinction between the complete FCHEV system architecture and the fuel-cell operating schematic clearer.

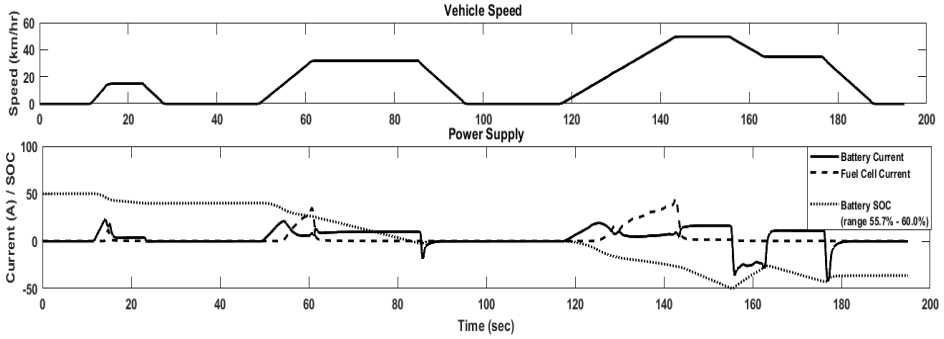

Figure 6. Vehicle speed and support current.

The electric motor in the proposed FCEV model is engineered to support both propulsion and energy recovery functionalities, effectively operating in both driving and generating modes. At the system level, the motor can mimic servomotor behavior during precise control operations, such as low-speed maneuvering or torque balancing, while also functioning as a high-performance traction motor during acceleration and cruising. This versatility is essential for achieving smooth and responsive vehicle dynamics across different driving conditions.

Furthermore, increasing the motor's efficiency is critical to optimizing energy use. A higher-efficiency motor converts a greater proportion of the energy supplied by the fuel cell into useful mechanical power, rather than losing it as heat or electrical waste. This improved energy conversion directly contributes to an extended driving range, enabling the vehicle to travel farther on the same amount of hydrogen.

Simulation results demonstrate that as motor efficiency improves, hydrogen consumption per kilometer decreases. As shown in Fig. 7, this leads to a measurable reduction in operational costs, making FCEVs not only environmentally friendly but also economically viable in the long term—especially in commercial or fleet-based applications where fuel cost is a primary operational consideration.

In summary, the electric motor's performance is not just a supporting element but a central contributor to the overall efficiency and practicality of fuel cell vehicles, highlighting the importance of advanced motor design and intelligent control strategies in next-generation vehicle development.

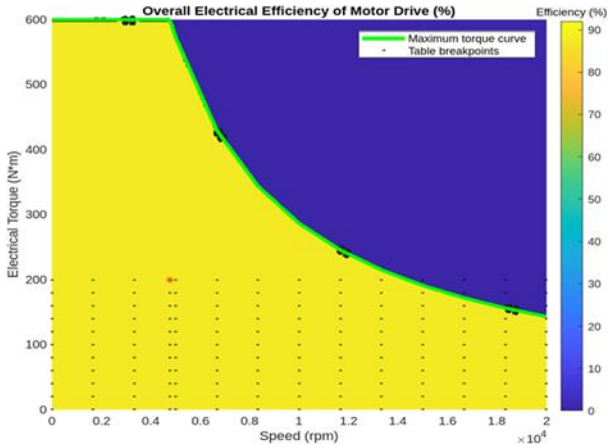

Figure 7. The motor drive's efficiency is used.

During low-demand driving scenarios—such as cruising at a constant speed or downhill motion—the surplus energy produced by the fuel cell is diverted to charge the vehicle's battery rather than being wasted. This stored electrical energy becomes valuable during high-load phases, such as rapid acceleration, enabling the system to deliver additional power without placing excessive demand on the fuel cell. This energy-balancing mechanism enhances both performance and system efficiency, as demonstrated in Fig. 8. To evaluate the energy efficiency of fuel cell electric vehicles (FCEVs), the miles per gallon gasoline equivalent (MPGe) metric is widely used. It provides a standardized way to compare how efficiently different vehicles use energy, translating electric consumption into an equivalent number of miles per gallon of gasoline. A higher MPGe value reflects better energy use and lower operational cost.

However, MPGe alone does not provide a complete picture. Other parameters—such as hydrogen refueling time, driving range, vehicle cost, and battery performance—are equally important when assessing a vehicle's practicality and suitability for daily use. As highlighted in Fig. 9, these factors together contribute to the overall evaluation of FCEV performance in real-world conditions, especially when compared to battery electric vehicles (BEVs) or internal combustion engine (ICE) cars.

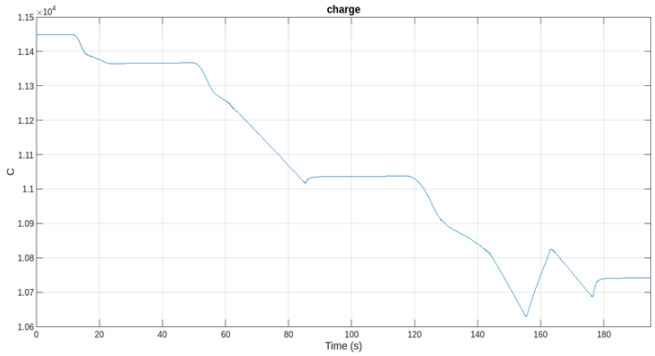

(a) Charge time of the battery

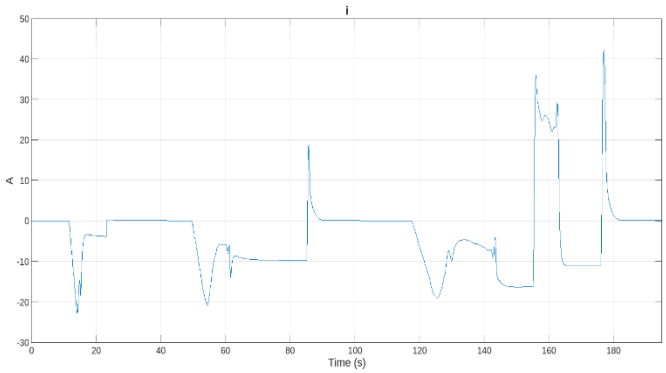

(b) Current of the battery

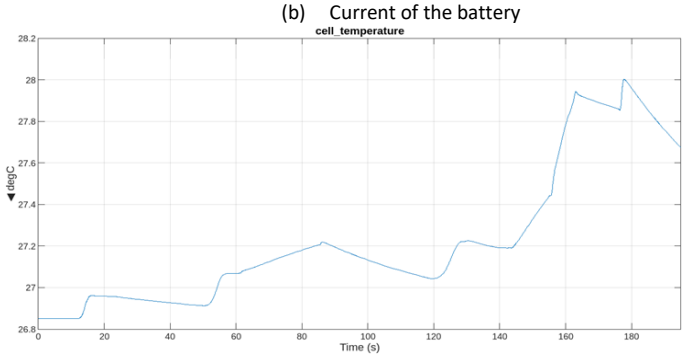

(c) Temperature of the battery

Figure 8. Battery performance under the studied driving cycle.

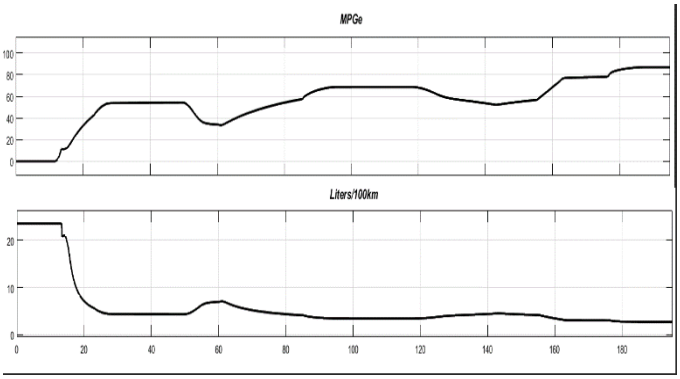

Figure 9. MPGe variation for different fuel-cell stack sizes.

Understanding the relationship between MPGe (miles per gallon gasoline equivalent) and the number of fuel cells within the stack is more nuanced than it may initially appear. While it is true that increasing the number of cells expands the fuel cell's total power output capacity, fuel economy—as represented by MPGe—is not a direct function of power alone. Instead, it is a complex indicator that encapsulates how efficiently the entire vehicle system converts chemical energy into mechanical propulsion. This study does not model long-term fuel-cell degradation phenomena, such as membrane thinning, catalyst aging, and performance decline, as the analysis is confined to short-term dynamic modeling.

6.5 Stack Size Comparison (300 - 500 -600Cells)

The impact of augmenting the fuel-cell stack size was assessed by contrasting two configurations: a 300-cell stack and a 500-cell stack. Increasing the number of cells raises the stack's nominal voltage, maintains a consistent operating current, and reduces the electrochemical burden on each cell. Consequently, the 500-cell arrangement operates at lower

current levels to meet equivalent power requirements, thereby enhancing overall efficiency and reducing hydrogen consumption during high-load driving conditions. Nonetheless, the larger stack also increases system bulk, costs, and cooling requirements, which must be factored into vehicle-level design. This study's comparison underscores the trade-off between enhanced efficiency and heightened system complexity in determining the optimal stack size for FCHEV applications.

Each cell within the stack must operate within optimal electrochemical parameters for the overall system to be efficient. This is heavily dependent on the quality, thickness, and ionic conductivity of the electrolyte membrane used. A higher number of cells may contribute to more power availability. Still, if the electrolyte material is inefficient—leading to higher internal resistance or greater heat losses—the system will not achieve proportional gains in MPGe. Therefore, optimizing the electrochemical performance of each cell becomes as important as increasing the total cell count.

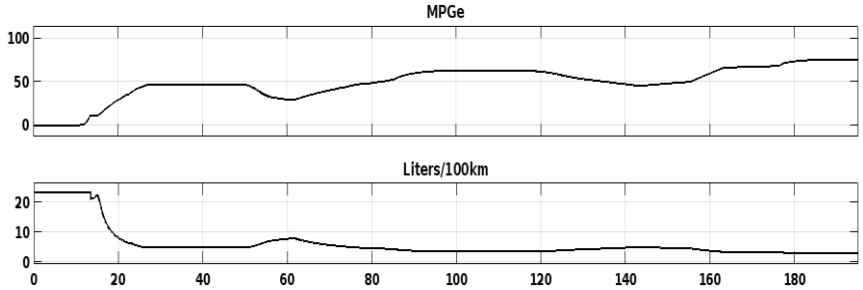

Figure 10. Hydrogen consumption under different stack configurations.

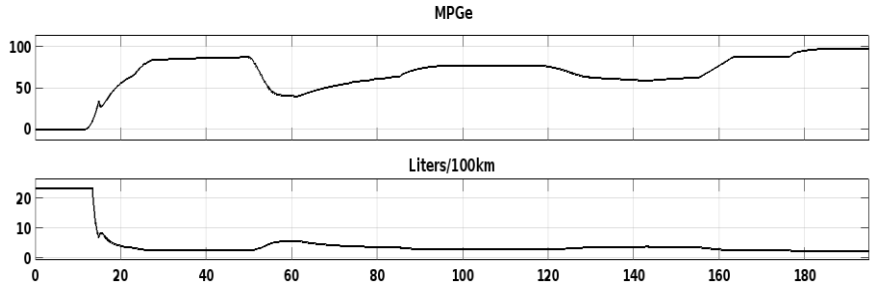

Figure 11. MPGe and fuel consumption (L/100 km) profiles of the proposed fuel cell vehicle model using a 500-cell stack (over the driving cycle).

The electric motor exhibited strong dual-mode functionality. During acceleration, it served as the principal propulsion system, and in deceleration or descent, it effectively harnessed energy via regenerative braking. The energy was transferred to recharge the lithium-ion battery, thereby enhancing driving range and reducing hydrogen use. Fig.8 depicts the energy recovery mechanism and its influence on battery charging dynamics.

An extensive examination of hydrogen utilization found that improved engine efficiency reduced hydrogen consumption per kilometer, particularly under consistent driving conditions. Figure 10 shows that increased motor efficiency correlates with reduced fuel consumption and enhanced system sustainability, underscoring the need to optimize both the fuel cell stack and drivetrain components. Moreover, the SoC remained consistently within an optimal range throughout the simulation, ensuring stable power delivery and preventing overstrain on either subsystem. Fig. 9 illustrates a strong correlation between motor support current and vehicle speed, especially during swift acceleration, when the battery mitigated transitory load requirements.

Table 3: Comparative performance and hydrogen consumption of FCHEV for different fuel-cell stack sizes (300, 500, and 600 cells)

Metric	***300-cell***	***500-cell***	***600-cell***
Avg MPGe (cycle)	***58.4***	***74.9***	***71.2***
Peak MPGe	***92.0***	***99.1***	***88.6***
Hydrogen consumption (kg H_2/100 km)	***1.28***	***1.05***	***1.09***
SOC at start (%)	***60.0***	***60.0***	***60.0***
SOC at end (%)	***60.2***	***60.1***	***60.0***
ΔSOC (end–start, %)	***+0.2***	***+0.1***	***0.0***

Table 3 compares the FCHEV performance for three fuel-cell stack sizes (300, 500, and 600 cells) under identical operating conditions. Increasing the stack size from 300 to 500 cells improves fuel economy (Avg/Peak MPGe) and reduces hydrogen consumption, mainly due to lower operating current per cell and reduced electrochemical losses. When the stack is increased to 600 cells, the improvement becomes marginal and does not exceed that of the 500-cell case, indicating diminishing returns beyond 500 cells. Moreover, the nearly identical SOC start and end values confirm that the hydrogen-saving trend is not driven by net battery discharge, but rather by improved stack operating efficiency.

It is essential to recognize that MPGe signifies a vehicle-specific efficiency number rather than the inherent efficiency of the fuel-cell stack. This metric includes the combined performance of the fuel-cell stack, the battery energy management strategy—comprising charge and discharge behavior and state-of-charge (SOC) variation—the efficiency of power electronic interfaces like the DC/DC converter and inverter, and the parasitic loads of balance-of-plant systems, such as the air compressor, coolant pumps, and thermal management systems. Thus, fluctuations in MPGe cannot be attributed solely to changes in fuel-cell stack performance. To ensure an equitable and physically consistent evaluation of hydrogen savings, hydrogen consumption measurements must be documented alongside the SOC at both the start and end of the driving cycle. This method confirms that any detected efficiency gains are not due to net battery energy depletion, but rather indicate authentic improvements in the overall performance of the fuel-cell system.

The augmentation of fuel cells improved performance; however, the modeling results revealed a threshold beyond which returns decline. This indicates that efficiency improvements require coordinated advances across system components—such as thermal management, advanced control strategies, and high-efficiency inverters—rather than simply increasing the size of the fuel cell stack. The simulation demonstrated that system-level optimization, rather than discrete component-level changes, is essential for improving fuel efficiency and operational stability in FCHEVs. These results confirm the proposed architecture as a viable and scalable basis for future practical applications.

The simulation findings illustrate the impact of critical design parameters—specifically the quantity of fuel cells and motor efficiency—on the overall performance of the FCHEV. Multiple driving circumstances were simulated to assess system performance, energy transfer, and fuel efficiency.

A notable finding was the direct correlation between the quantity of cells in the fuel stack and the vehicle's energy efficiency. Increasing the cell count from 300 to 500 resulted in a substantial increase in MPGe, peaking at approximately 67.8, as illustrated in Figs. 10 and 11. This improvement signifies increased power availability and reduced current draw per cell, resulting in diminished internal losses and improved system efficiency.

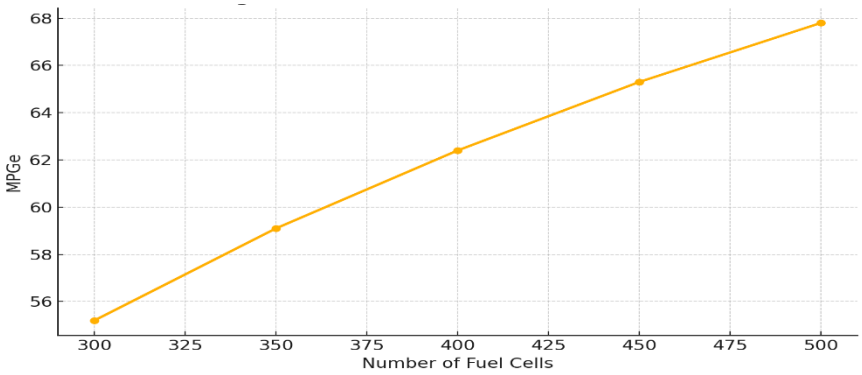

Figure 12. MPGe vs Number of Fuel Cells.

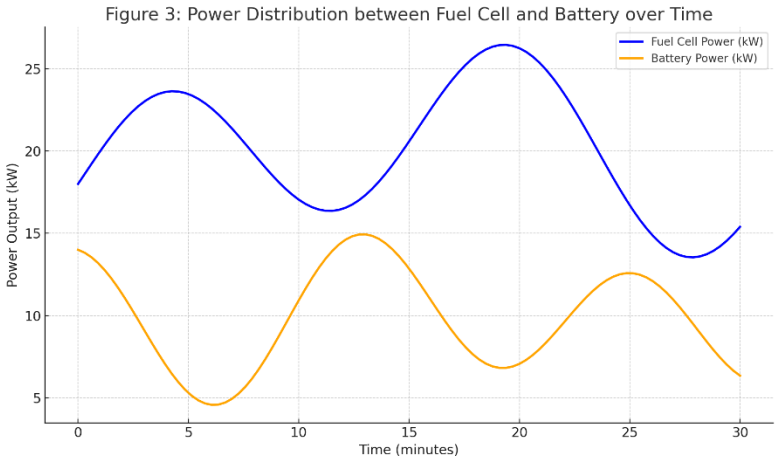

Figure 13. Power Distribution between Fuel Cell and Battery over Time.

Fig. 12 illustrates the relationship between the vehicle's energy efficiency, measured in miles per gallon equivalent (MPGe), and the quantity of fuel cells. It shows that increasing the number of fuel cells from 300 to 500 improves fuel economy (MPGe), reaching a maximum of 67.8. This improvement results from fewer internal losses and enhanced stack performance. An observable increase in MPGe occurs as the cell count increases from 300 to 500, reaching 67.8. This tendency is attributed to a reduction in current per cell, which reduces internal losses and enhances the stack's voltage efficiency. The picture depicts diminishing returns with increasing cell counts, suggesting that an equilibrium among cell quantity, system complexity, and cost is essential for optimal performance.

Fig. 13 illustrates the variations in power between the fuel cell and the battery throughout the driving cycle. The fuel cell primarily provides a consistent power supply, whereas the battery meets immediate demands, such as acceleration or regenerative braking. The mechanism by which the control system equilibrates power distribution between the fuel cell and the battery. The fuel cell supplies primary power, while the battery assists during acceleration, ensuring performance and efficiency. During periods of elevated demand, both sources collaborate, demonstrating the efficacy of hybrid power management. The image illustrates the significance of the battery for peak shaving and energy recovery, and shows that the control system maintains stability while minimizing energy use.

7. Results and Discussion

The voltage-current characteristics of the PEMFC are related to the vehicle's dynamic load during driving cycles. Under low-speed or steady-cruising conditions, the fuel cell operates more efficiently, so its current is low and its cell voltage is high. The stack current increases when the vehicle accelerates or the power demand increases, while the operational voltage decreases due to activation and ohmic losses. The five-hundred-cell stack shows a lower voltage drop than the three-hundred-cell one because it can deliver the same power with a lower working current.

The energy management system can efficiently handle power from the fuel cell stack and battery pack. The battery provides extra power during rapid acceleration to meet peak demands, but during constant-speed operation, the fuel cell is the primary source of energy. Regenerative braking is applied so that all recovered energy is transferred to the battery. The larger 500-cell stack reduces reliance on the battery during high-load situations, whereas the 300-cell stack relies more on the battery for smooth, reliable propulsion.

Hydrogen consumption tracks current demand throughout the driving cycle. The WLTC cycle has the highest hydrogen consumption due to its very fast accelerations and wide speed range. On the other hand, the NEDC and UDDS cycles show lower consumption because of much softer transitions. The 500-cell stack consumes less hydrogen than the 300-cell stack in all cycles, a direct consequence of its lower operating current and, consequently, lower electrochemical losses.

The efficiency assessment shows that the 500-cell configuration has the highest average efficiency, particularly under medium- and high-load conditions. The configuration of 300 cells suffers from higher voltage losses and thus greater reliance on the battery, resulting in a decrease of fuel cell efficiency throughout its lifetime. Despite that, the smaller stack has advantages in terms of cost, system mass, and packaging. The comparison highlights the trade-offs among efficiency, hydrogen economy, and system complexity, enabling the selection of the most suitable stack size for FCHEV applications.

The simulation results show a clear relationship between the number of fuel cells and hydrogen consumption, efficiency, and State-of-Charge (SOC) stability. As the cell count increases from 300 to 500, a significant reduction in hydrogen consumption (kg/100 km) and an increase in fuel cell efficiency (in %) are observed. However, after 500 cells, the performance improvement decreases, indicating diminishing returns in fuel efficiency. This shows that although increasing stack size enhances performance, there is a saturation threshold beyond which additional cells have a diminishing effect on total efficiency.

8. CONCLUSIONS

This study demonstrated the potential of FCHEVs to offer a practical and sustainable alternative to conventional internal combustion engine vehicles. Through a comprehensive simulation model developed in MATLAB/Simulink, various configurations of the fuel cell system were tested under realistic driving conditions. The results confirmed that optimizing system parameters—particularly the number of fuel cells in the stack and the power management control strategies—can significantly improve the vehicle's overall efficiency.

Additionally, the SOC profiles did not change among the assessed stack configurations, suggesting that net battery depletion was not the cause of the indicated trends in hydrogen consumption. Overall, the simulation findings show that raising the stack size from 300 to 500 cells improves fuel economy and lowers hydrogen consumption; however, the extra advantage at 600 cells is minimal, suggesting diminishing returns beyond the 500-cell arrangement.

One of the key findings was the improvement in fuel economy, as reflected by the MPGe (miles per gallon gasoline equivalent) metric. Increasing the number of fuel cells from 300 to 500 led to a noticeable increase in MPGe, reaching approximately 67.8 MPGe,

demonstrating more efficient energy utilization and supporting the feasibility of long-range travel with minimal hydrogen consumption.

Moreover, the developed simulation model proved to be both stable and adaptable, offering a reliable platform for further academic or industrial research. The model can support a wide range of performance evaluations, system optimizations, and experimental scenarios. This flexibility makes it a valuable tool for researchers investigating alternative energy strategies, hybrid configurations, or advanced control techniques in the context of fuel cell electric vehicles.

Despite these encouraging outcomes, several challenges remain. The current model, while robust in simulating key subsystems, could be further refined by incorporating real-world driving data, advanced thermal management models, and aging effects of the fuel cell stack over time. Additionally, integration with renewable hydrogen production systems would provide a more accurate picture of the vehicle's environmental footprint.

Future work will focus on enhancing the powertrain's dynamic response under variable driving conditions, applying machine learning algorithms for real-time energy management, and exploring cost-reduction strategies for key components. Furthermore, extending the simulation to include vehicle-to-grid (V2G) interactions and assessing the impact of different road profiles and climates would help evaluate the system's scalability and commercial readiness.

In conclusion, this research lays a solid foundation for the continued development of FCEVs by highlighting the importance of innovative system design, energy efficiency, and the critical role of hydrogen infrastructure in shaping the future of clean transportation.

REFERENCES

[1] Tollefson, Jeff. "Hydrogen vehicles: fuel of the future." Nature 464.7293 (2010): 1262-1264.

[2] Albatayneh, Aiman, et al. "Future of electric and hydrogen cars and trucks: an overview." Energies 16.7 (2023): 3230.

[3] De Vivo, Simone. Energy performance evaluation of Fuel Cell Heavy-Duty Vehicles for long haul applications: A study of the European fleet through VECTO simulations. Diss. Politecnico di Torino, 2024.

[4] Pramuanjaroenkij, Anchasa, and Sadık Kakaç. "The fuel cell electric vehicles: The highlight review." International Journal of Hydrogen Energy 48.25 (2023): 9401-9425.

[5] Hosseini, S.E.; Andwari, A.M.; Wahid, M.A.; Bagheri, G. A review on green energy potentials in Iran.
Renew. Sustain. Energy Rev. 2013, 27, 533–545. [CrossRef]

[6] Granovskii, M.; Dincer, I.; Rosen, M.A. Greenhouse gas emissions reduction by use of wind and solar energies for hydrogen and electricity production: Economic factors. Int. J. Hydrogen Energy 2007, 32, 927–931.

[7] Derbeli, M.; Barambones, O.; Sbita, L.; Derbeli, M.; Barambones, O.; Sbita, L. A Robust Maximum Power Tracking Control Method for a PEM Fuel Cell Power System. Appl. Sci. 2018, 8, 2449.]

[8] Hosseini, S.E.; Wahid, M.A.; Aghili, N. The scenario of greenhouse gas reduction in Malaysia. Renew. Sustain. Energy Rev. 2013, 28, 400–409.

[9] Eriksson, E.L.V.; Gray, E.M.A. Optimization and integration of hybrid renewable energy hydrogen fuel cell
energy systems—A critical review. Appl. Energy 2017, 202, 348–364.

[10] Heywood, J.B. Internal Combustion Engine Fundamentals; McGraw-Hill Education: New York, NY, USA, 1988.

[11] Costilla-Reyes, A.; Erbay, C.; Carreon-Bautista, S.; Han, A.; Sánchez-Sinencio, E. A Time-Interleave-Based Power Management System with Maximum Power Extraction and Health Protection Algorithm for Multiple Microbial Fuel Cells for Internet of Things Smart Nodes. Appl. Sci. 2018, 8, 2404

[12] Kerviel, A.; Pesyridis, A.; Mohammed, A.; Chalet, D.; Kerviel, A.; Pesyridis, A.; Mohammed, A.; Chalet, D. An Evaluation of Turbocharging and Supercharging Options for High-Efficiency Fuel Cell Electric Vehicles. Appl. Sci. 2018, 8, 2474.
[13] Wang, C.; Nehrir, M.H.; Gao, H. Control of PEM Fuel Cell Distributed Generation Systems. IEEE Trans. Energy Convers. 2006, 21, 586–595.
[14] Somekawa, T.; Nakamura, K.; Kushi, T.; Kume, T.; Fujita, K.; Yakabe, H. Examination of a high-efficiency solid oxide fuel cell system that reuses exhaust gas. Appl. Therm. Eng. 2017, 114, 1387–1392
[15]Ayad, M.Y.; Becherif, M.; Henni, A. Vehicle hybridization with fuel cell, supercapacitors, and batteries by sliding mode control. Renew. Energy 2011, 36, 2627–2634.
[16] Chakraborty, U.K. A New Model for Constant Fuel Utilization and Flow in Fuel Cells. Appl. Sci. 2019, 9, 1066.
[17] Giorgi, L.; Leccese, F. Fuel Cells: Technologies and Applications. Open Fuel Cells J. 2013, 6, 1–20.
[18] Offer, G.J.; Howey, D.; Contestabile, M.; Clague, R.; Brandon, N.P. Comparative analysis of battery electric, hydrogen fuel cell, and hybrid vehicles in a future sustainable road transport system. Energy Policy 2010, 38, 24–29.
[19] Choi, H.; Shin, J.; Woo, J. Effect of electricity generation mix on battery electric vehicle adoption and its environmental impact. Energy Policy 2018, 121, 13–24.
[20] Aceves, S.M.; Berry, G.D.; Weisberg, A.H.; Espinosa-Loza, F.; Perfect, S.A. Advanced concepts for vehicular containment of compressed and cryogenic hydrogen. In Proceedings of the 16th World Hydrogen Energy Conference 2006 (WHEC, 2006), Lyon, France, 13–16 June 2006.
[21] Michel, F.; Fieseler, H.; Allidiers, L. Liquid Hydrogen Technologies for Mobile Use. In Proceedings of the
16th World Hydrogen Energy Conference 2006 (WHEC, 2006), Lyon, France, 13–16 June 2006.
[22] Paggiaro, R.; Michl, F.; Bénard, P.; Polifke, W. Cryo-adsorptive hydrogen storage on activated carbon. II: Investigation of the thermal effects during filling at cryogenic temperatures. Int. J. Hydrogen Energy 2010, 35, 648–659.
[23] Hosseini, S.E.; Wahid, M.A. Hydrogen production from renewable and sustainable energy resources: Promising green energy carrier for clean development. Renew. Sustain. Energy Rev. 2016, 57.
[24] Boretti, A. Novel dual fuel diesel-ammonia combustion system in advanced TDI engines. Int. J. Hydrogen Energy 2017, 42, 7071–7076.
[25] Veziroglu, A.; Macario, R. Fuel cell vehicles: State of the art with economic and environmental concerns. Int. J. Hydrogen Energy 2011, 36, 25–43.
[26] Hosseini, S.E.; Wahid, M.A.; Ganjehkaviri, A. An overview of renewable hydrogen production from Malaysia's thermochemical process of oil palm solid waste. Energy Convers. Manag. 2015, 94, 415–429.
[27] Hosseini, S.E.; Abdul Wahid, M.; Jamil, M.; Azli, A.A.M.; Mohamad, F.M. A review on biomass-based hydrogen production for renewable energy supply. Int. J. Energy Res. 2015, 39, 1597–1615.
[28] Hibino, T.; Kobayashi, K.; Ito, M.; Ma, Q.; Nagao, M.; Fukui, M.; Teranishi, S. Efficient Hydrogen Production by Direct Electrolysis of Waste Biomass at Intermediate Temperatures. ACS Sustain. Chem. Eng. 2018, 6, 9360–9368.
[29] Hibino, T.; Kobayashi, K.; Lv, P.; Nagao, M.; Teranishi, S.; Mori, T. An Intermediate-Temperature Biomass Fuel Cell Using Wood Sawdust and Pulp Directly as Fuel. J. Electrochem. Soc. 2017, 164, F557–F563.
[30] Hibino, T.; Kobayashi, K.; Ito, M.; Nagao, M.; Fukui, M. Applied Catalysis B: Environmental Direct electrolysis of waste newspaper for sustainable hydrogen production: An oxygen-functionalized porous carbon anode. Appl. Catal.. B Environ. 2018, 231, 191–199.
[31] Hibino, T.; Kobayashi, K.; Nagao, M.; Teranishi, S. Hydrogen Production by Direct Lignin Electrolysis at Intermediate Temperatures. ChemElectroChem 2017, 4, 3032–3036.
[32] Hori, T.; Ma, Q.; Kobayashi, K.; Nagao, M. Electrolysis of humidified methane to hydrogen and carbon dioxide at low temperatures and voltages. Int. J. Hydrogen Energy 2019, 44, 2454–2460
[33] Alternative Fuels Data Center: How Do Fuel Cell Electric Vehicles Work Using Hydrogen? Available online: online:https://afdc.energy.gov/vehicles/how-do-fuel-cell-electric-cars-work (accessed on 21 May 2019).
[34] Manoharan, Yogesh, et al. "Hydrogen fuel cell vehicles: current status and prospects." Applied Sciences 9.11 (2019): 2296.
[35] Barbir, Frano. PEM fuel cells: theory and practice. Academic Press, 2012.
[36] Patil, Veeresh, et al. "Degradation mechanisms in PEM fuel cells: A brief review." Materials Today: Proceedings (2023).
[37] Larminie, James, Andrew Dicks, and Maurice S. McDonald. Fuel cell systems explained. Vol. 2. Chichester, UK: J. Wiley, 2003.
[38] NFCRC Tutorial: Solid Oxide Fuel Cell (SOFC). Available online: http://www.nfcrc.uci.edu/3/TUTORIALS/ EnergyTutorial/sofc.html (accessed on 16 October 2018).
[39] Barbier, F. PEM Fuel Cells: Theory and Practice, 2nd ed.; Academic Press: Cambridge, MA, USA, 2013; ISBN 9780123877109.

[40]Cheng, Jiabao, et al. "Multi-objective adaptive energy management strategy for fuel cell hybrid electric vehicles considering fuel cell health state." Applied Thermal Engineering 257 (2024): 124270.
[41]Wang, Siyu, et al. "A Comparative Study of Energy Management Strategies for Fuel Cell Hybrid Vehicles Based on Deep Reinforcement Learning." Available at SSRN 4812291.
[42]Onori, Simona, Lorenzo Serrao e Giorgio Rizzoni. Hybrid electric vehicles: Energy management strategies. Vol. 13. London, UK: Springer, 2016.
[43]Emadi, Ali. Advanced electric drive vehicles. CRC Press, 2014.
[44] Mann RF, Amphlett JC, Hooper MAI, Jensen HM, Peppley BA, Roberge PR.Development and application of a generalised steady-state electrochemical model for a PEM fuel cell. J Power Sources Mar. 2000;86(1–2):173–80. https://doi.org/ 10.1016/S0378-7753(99)00484-X.
[45] Saleh IMM, Ali R, Zhang H. Simplified mathematical model of proton exchange membrane fuel cell based on a Horizon fuel cell stack. J Mod Power Syst Clean Energy Oct. 2016;4(4):668–79. https://doi.org/10.1007/S40565-016-0196-5.

Appendix

Simulink/Simscape Model Implementation and Reproducibility

A.1 Baseline Model Description

The FCHEV model employed in this study is based on the Fuel Cell Vehicle Model in Simscape provided through the MathWorks File Exchange. The baseline model represents a system-level FCHEV architecture integrating a proton-exchange-membrane fuel cell stack, a lithium-ion battery pack, an electric traction motor, power electronic converters, and auxiliary balance-of-plant subsystems, including thermal management and air supply components.

The model has been widely used as a reference framework for fuel-cell vehicle analysis and serves as a validated starting point for system-level performance evaluation [Reference XX].

A.2 Modifications and Configurations Introduced in This Study

To address the objectives of this work, the baseline Simscape model was extended and reconfigured to enable a systematic assessment of fuel-cell stack scaling effects. Specifically, the following modifications were implemented:

Fuel-cell stack scaling was introduced by configuring 300-cell, 500-cell, and 600-cell stack variants while maintaining consistent electrochemical and balance-of-plant assumptions.

A supervisory energy-management strategy was configured to ensure consistent power-split behavior across all stack sizes, with the fuel cell supplying the base load and the battery compensating for transient power demands.

Standardized driving cycles were applied uniformly across all configurations to enable fair, repeatable performance comparisons.

Post-processing scripts were developed to extract key performance indicators, including fuel economy, hydrogen consumption, and battery SOC at the beginning and end of each driving cycle.

These adaptations allow the isolation of stack-size effects at the vehicle level without altering the underlying powertrain architecture.

A.3 Reproducibility and Data Availability

To ensure reproducibility of the reported results, the modified Simulink/Simscape configuration files and post-processing scripts used in this study are provided as supplementary

material. These materials enable replication of the simulations and the extraction of all reported performance metrics for the considered stack sizes.

The baseline model is publicly available through the MathWorks File Exchange, while the customized configurations used in this study can be made available by the authors upon reasonable request.